Electrokinetic and optical control of bacterial microrobots

2011 J. Micromech. Microeng. 21 035001

(http://iopscience.iop.org/0960-1317/21/3/035001)

J. Micromech. Microeng. **21** (2011) 035001 (8pp) doi:10.1088/0960-1317/21/3/035001

Electrokinetic and optical control of bacterial microrobots

Edward B Steager[1,2,3], Mahmut Selman Sakar[2,3], Dal Hyung Kim[1], Vijay Kumar[2], George J Pappas[2] and Min Jun Kim[1]

[1] Department of Mechanical Engineering and Mechanics, Drexel University, Philadelphia, PA 19104, USA
[2] GRASP Laboratory, School of Engineering and Applied Sciences, Philadelphia, PA 19104, USA

E-mail: mkim@coe.drexel.edu

Received 14 September 2010, in final form 1 December 2010
Published 1 February 2011
Online at stacks.iop.org/JMM/21/035001

Abstract
One of the great challenges in microscale science and engineering is the independent manipulation of cells and man-made objects on the micron scale. For such work, motile microorganisms are integrated with engineered systems to construct microbiorobots (MBRs). MBRs are negative photosensitive epoxy (SU-8) microfabricated structures with typical feature sizes ranging from 1 to 100 μm coated with a monolayer of swarmer cells of the bacterium *Serratia marcescens*. The adherent cells naturally coordinate to propel the microstructures in fluidic environments. In this study, ultraviolet light is used to control rotational motion and direct current electric fields are used to control the two-dimensional movement of MBRs. They are steered in a fully automated fashion using computer-controlled visual servoing, used to transport and manipulate micron-sized objects, and employed as cell-based biosensors. This work is a step toward *in vitro* mechanical or chemical manipulation of cells as well as controlled assembly of microcomponents.

S Online supplementary data available from stacks.iop.org/JMM/21/035001/mmedia

(Some figures in this article are in colour only in the electronic version)

1. Introduction

There is a need for controllable actuators to accomplish tasks including single cell manipulation and microassembly [1–6]. It is well understood that non-reciprocal movements are necessary for propulsion in low Reynolds number fluidic environments, and bio-inspired devices based on the helical shape of the bacterial flagellum or the shape-varying stroke of the eukaryotic flagellum have garnered considerable attention [7–13]. Such biomimetic microactuators can be manufactured using inorganic materials; however, the ability to fabricate the required geometries is practically limited by the planar nature of microfabrication processes. Using biomolecular motors is another option, but these systems are difficult to employ when isolated from the supporting cells [14, 15]. As an alternative solution, previous studies explored different forms of actuation and control with microorganisms [16–22]. Bacteria, in particular, offer several advantages as controllable microactuators: they draw chemical energy directly from their environment, they can be genetically engineered and employed as sensing elements [23] and they are scalable and configurable in that the cells can be selectively patterned [24].

Bacteria are a key component of several hybrid organic/inorganic MEMS devices, including a host of actuators and sensors. In one of the first instances of biointegrated, mechanical actuators, microscale rotors were driven using the gliding bacteria *Mycoplasma mobile*, which were directionally attached to the rotor teeth [16]. Lab-on-a-chip fluid pumping and mixing was also demonstrated with *Serratia marcescens* and *Escherichia coli*, respectively [25, 26]. The chaotic interactions of swimming bacteria with microscale gears have also been shown to produce useful work given the proper choice of device geometry [27, 28].

Much of the current work on harnessing the mechanical energy of bacteria has been directed by researchers with interest in robotic microassembly. As such, there has been

[3] These authors contributed equally to this work.

a focus on the ability to control groups of cells with the goal of directing and harnessing their energy to accomplish tasks such as manipulation and assembly. Magnetotactic bacteria may be controlled to swim *en masse* in the direction of magnetic field lines and have been used as collectives to move microscale structures [18]. On/off microbead propulsion in response to chemical stimulus has been demonstrated using the bacterium *S. marcescens* [19], but controlled actuation in response to chemical gradients is inherently limited by the development of the chemical concentrations, as governed by the diffusion equation. On/off control of microstructure movement powered by swarming *S. marcescens* has also been investigated using short-term exposure to ultraviolet light [20].

For the specific application of automatic, remotely controlled manipulation of cells or microobjects, control of both rotation and translation is desired. Rotational control is of particular interest where the device has a nonsymmetrical geometry designed for engagement and trapping. Since many potential applications for micromanipulation are performed on a glass slide in a single focal plane using standard light microscopy, the manipulation techniques presented in this work are restricted to two-dimensional planar motion.

In this paper we investigate an alternative solution for the controlled manipulation of microscale components with a biointegrated approach. Bacteria attached to the surface of microfabricated parts, referred to as microbiorobots (MBRs), are shown to naturally impart a predominantly rotational motion, largely due to the distribution of bacterial cell body orientations and hence flagellar thrusts [29]. We show that the rate of rotation can be *predictably* adjusted using optical stimulus and demonstrate two-dimensional control of MBRs using electric fields to harness the electrical potential of the cells. The control techniques are applied to orient and steer bacterial microbiorobots as well as to transport target loads. The ability to monitor the behavior of these robots in response to biologically relevant chemicals is an important requirement for further development; therefore, we also demonstrate that integrated live cells can be employed as sensing elements using copper ions as an example.

2. Results and discussion

The synthetic component of the MBR is fabricated out of SU-8 (figure 1), which is biocompatible, patternable in a wide range of shapes and thicknesses, and is only slightly denser than the working fluid. The bacteria *S. marcescens* were cultured using a swarm plate technique (L-broth containing 0.6% Difco Bacto-agar and 5 g l^{-1} glucose) [17]. They are hyperflagellated, elongated and migrate cooperatively [30]. The polysaccharide-rich pink slime produced by swarmer cells of *S. marcescens* enables them to stick to the surface of the microstructures [31]. Bacteria were attached by blotting directly along the active swarm edge and readily adhered to the SU-8 microstructures, generally covering more than 90% of the surface (figure 2(*a*)). Using a water-soluble sacrificial dextran layer [32], hundreds of MBRs were released into the fluidic chamber without causing structural damage (see section 3). Greater than 90% of properly fabricated

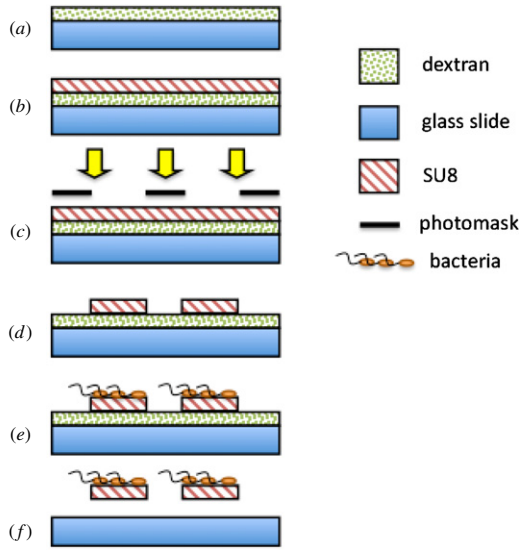

Figure 1. Microfabrication of biocompatible SU-8 microstructures. (*a*) The glass slide is coated with Dextran. (*b*) The SU-8 layer is spin coated onto the sacrificial dextran layer. (*c*) UV light is transmitted through a photomask to create an exposure pattern. (*d*) SU-8 photoresist is developed. (*e*) Sections of the glass slide each with many microstructures are inverted along the swarm edge for bacterial attachment. (*f*) Individual microstructures are released into the motile buffer.

MBRs move upon release from the substrate. An analysis of the orientation of the attached bacteria showed local correlation. With a fluorescent labeling technique, it was observed that the flagella were free to move even though the cell bodies were fixed (movie S1 available online at stacks.iop.org/JMM/21/035001/mmedia).

Electric fields (EF) were applied to the MBRs in a custom-designed galvanotaxis chamber via agar salt bridges, Steinberg's solution and graphite electrodes (see section 3). The design minimizes the adverse effects of electrode byproducts while keeping the pH and temperature relatively constant (±1 °C) inside the control chamber. The control chamber was filled with a standard cell motility buffer solution. Observations were performed in the central portion of the control chamber where dielectrophoretic effects due to field nonlinearities are minimized.

2.1. Electrokinetic characterization

MBRs were initially tested without external stimuli, that is, with no electric field or ultraviolet (UV) light. The MBRs were free to move inside the fluid, and their movement due to bacterial actuation was immediately observed. This collective response is due to flagellar actuation of the adherent bacteria and results in translation of the center of mass combined with rotation (figure 2(*b*)). We call this *self-actuation*. As a control, the SU-8 microstructures without bacteria attached were tested in the galvanotaxis chamber by applying direct current (dc) electric fields (EFs) ranging from 1 to 10 V cm^{-1}. During these experiments, the structures demonstrated no movement as expected. Next, EFs ranging from 1 to 10 V cm^{-1} were applied to the MBRs. They responded by moving toward

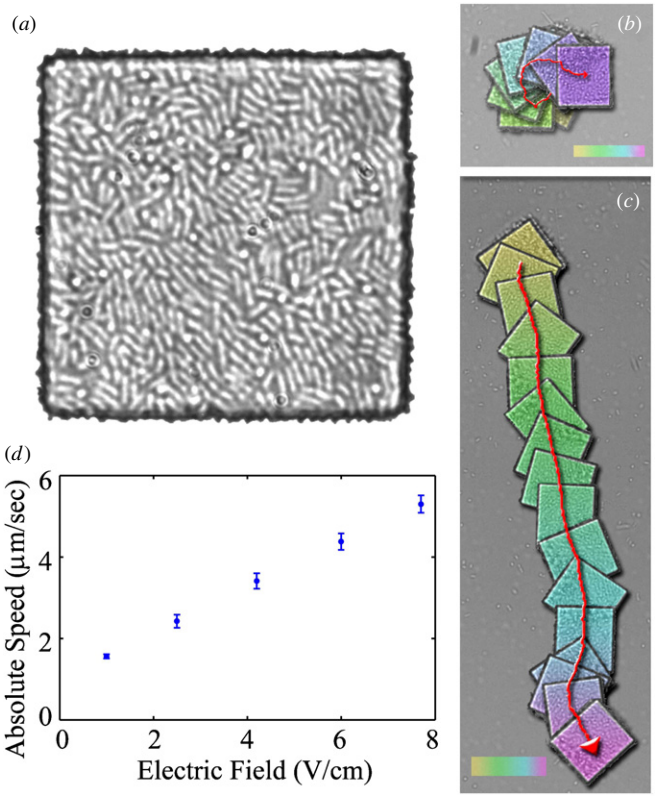

Figure 2. Microbiorobot self-actuation and electrokinetic response. (*a*) Phase contrast image of 40 × 40 μm^2 MBRs with the bacterial carpet monolayer. (*b*) Shown in this time-lapse image, the coordination of bacterial flagella leads to self-actuation of the MBR resulting in a net rotation and translation. (*c*) Upon application of electric fields the MBRs exhibit increased translational movement; however, the component due to self-actuation is superimposed on this translational motion. (*d*) MBR speed is directly proportional to the applied electric field which shows that electrophoresis is the dominant electrokinetic phenomenon. The component of speed due to self-actuation is evident from the *y*-intercept of the best-fit line. The color-coded bars represent time evolution (30 s) as well as length scale (50 μm).

the positive electrode. Upon switching the polarity of the system, the motion reversed direction in less than 30 ms. The linear movement was manifested as an additional component of the velocity. The component due to the self-coordination of bacteria remained active during the application of electric fields (figure 2(*c*)).

To investigate the fundamental electrokinetics of the microbiorobot, several trials were performed by measuring velocity versus the electric field. This investigation yielded a linear relationship between the two variables reflective of electrophoresis with a measured electrophoretic mobility of 0.56 μm cm s^{-1} V^{-1} (figure 2(*d*)). The result was consistent over all bacterial swarm cultures. This value implies that MBRs may be useful to perform tasks in the typical field of view of light microscopes at low applied voltages. The detailed motion of the microbiorobot was accurately modeled by a sum of the movement due to self-actuation and electrophoretic actuation. Indeed, surface patterning of bacteria imparted a charge that leads to a direct mechanism to control the motion of MBRs. Previous work showed that electrolysis can cause a change of the pH level especially around the electrodes which in turn triggers a chemotactic response in bacteria [33]. However, it should be noted that the directed movement we observed is not chemotactic, as the response times of the MBRs were considerably shorter ($\ll$1s) than the time necessary for the development of gradients of chemoeffectors by diffusion.

Experiments with individual bacteria showed that the movement is electrophoresis caused by the inherent charge of the bacterial cells rather than galvanotaxis, a directed response arising from the thrust of the bacterial flagella. Galvanotaxis in bacteria is caused by a difference in electrophoretic mobility between the cell body and flagellum [34]. Unlike previous observations made on swimming cells of *E. coli* and *Salmonella typhimurium*, swarmer cells of *S. marcescens* did not align themselves along the applied electric fields. The results of experiments designed to study the fundamental electrokinetics of individual bacteria (see section 3) indicated that there was not a significant effect of electric fields on the orientation of *S. marcescens* for the experimental conditions of this research, with a uniform distribution of orientations across the range of angles and applied electric fields. This would imply that there is not a significant difference in electrophoretic mobility between the flagella and the cell body. As electric fields were applied, cells were pulled toward the positive electrode. However, the orientations of the individual cell bodies were not affected. Thus, the overall velocity vector for the cells could be decomposed into the velocity due to the thrust of the swimming bacterium and the electrophoretic component. The bulk cell movement is electrophoretic in nature due to negative surface charge. It should be emphasized that the cells in this study were swarm cells taken directly from the agar plate to reflect the morphology of the cells blotted on the MBRs.

2.2. Photoresponse

Exposure to UV light has been established as a mechanism which affects the motility of bacteria [35]. Since MBRs generally exhibit rotational motion in the absence of external stimuli, UV light exposure is an effective means of adjusting angular velocity or completely stopping rotational motion [20]. Several trials were performed to characterize the UV response. Video was first captured for 10 s to record unexposed motion and was continuously recorded during three subsequent 5 s exposures. The optical path included a 100 W Hg light source and a 63× PL Fluorotar objective. The orientation of the MBRs was tracked and evaluated in MATLAB using a feature-based tracking algorithm [36]. While each individual trial had significant differences in initial angular velocity, and minor fluctuations in angular velocity during exposure, it was discovered that the general behavior was quite similar between trials, and three distinct regions could summarize motion (figure 3). As expected, between 0 and 10 s angular velocity was relatively constant since no stimulus had been applied. After the initial exposure to UV light, the rotational motion nearly ceased for 1–2 s before resuming at a lower angular velocity. It is hypothesized that this initial cessation may be related to the brief induction of tumbling in the bacteria

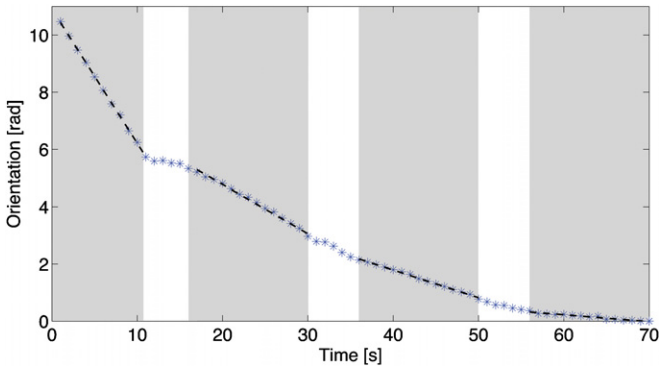

Figure 3. Characterization of the effect of photoexposure on angular orientation. Shown are the averaged results from several trials of exposure of MBRs to UV light, as well as trend lines between UV exposures. The white regions represent UV exposure. The final data point (70 s) was normalized as zero radians for all trials to reveal characteristic trends. Note that the slope of this curve represents angular velocity.

as the cells adjust to the stimulus [35, 37]. Subsequent exposures further decreased the angular velocity without the cessation phenomena. Between the subsequent exposures, angular velocity remained constant at the decreased levels. This characterization was used to temporarily stop rotation and adjust angular orientation of MBRs for later microtransport experiments.

To determine if photoexposure affects the electrokinetic reponse of MBRs, we repeated our characterization procedure by applying electric fields (ranging from 1 to 10 V cm^{-1}) to MBRs after deactivating them using UV light. The MBRs demonstrated the same electrophoretic movement as before the exposure, and as expected, the movement due to self-coordination of the bacterial carpet was completely missing.

2.3. Microtransport

As a demonstration of the ability to steer MBRs, microscale C-shaped parts that we call goals were fabricated using standard lithography and SU-8 photoresist. The goals were released in the control chamber along with square-shaped MBRs measuring 40 μm on each side. By varying the direction of the electric field, the MBRs were easily steered through the entrance of the goals even while continually rotating (figure 4(*a*)).

As an exhibit of directional control, a line-tracking experiment was designed. A simple path defining the letters 'UP' was fed to a feedback control algorithm that uses estimates of the current location of the MBR and the error with respect to the predefined trajectory to control the EF (figure 4(*b*)). The MBR was tracked using an image-processing algorithm, and visual feedback control was demonstrated (figure 4(*c*)). The overall performance can be easily improved by using a more sophisticated control algorithm.

Coupling the light and electric field mechanisms together enables control over the angular orientation as well as two-dimensional positioning of the MBR. A task was assigned of transporting a cube-shaped target load measuring 10 μm on each side using a U-shaped MBR referred to as a transporter, which was positioned and oriented using a combination of bacterial self-actuation, electrokinetics and photoexposure

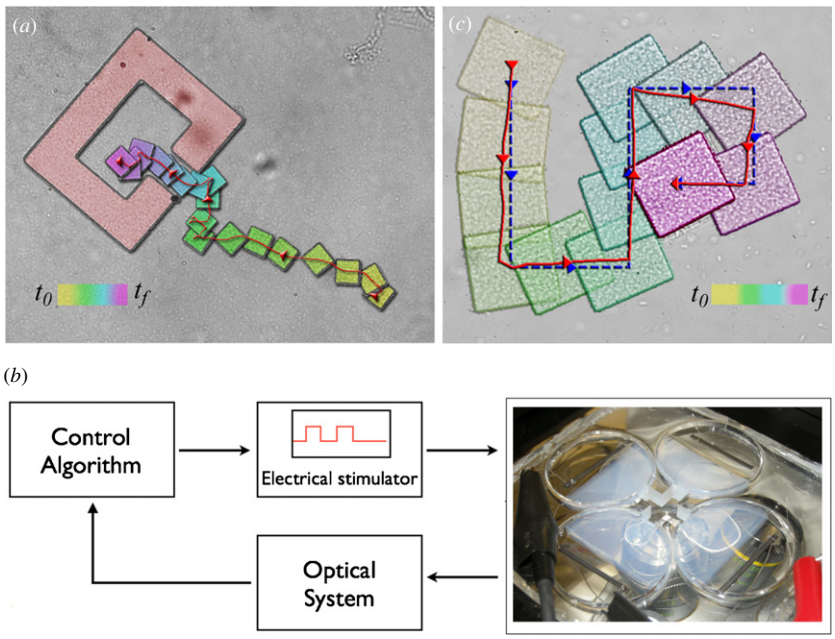

Figure 4. MBR control. (*a*) An MBR is directed through the entrance of a C-shaped microfabricated goal using teleoperation (movie S2 available online at stacks.iop.org/JMM/21/035001/mmedia). Scale bar represents time (2 min) as well as length (100 μm). (*b*) Block diagram for vision-based computer control of MBRs with a picture of the experimental setup. (*c*) Using a feedback control algorithm, an MBR is steered along a specified path (movie S3 available online at stacks.iop.org/JMM/21/035001/mmedia). Scale bar represents time (1 min) as well as length (50 μm).

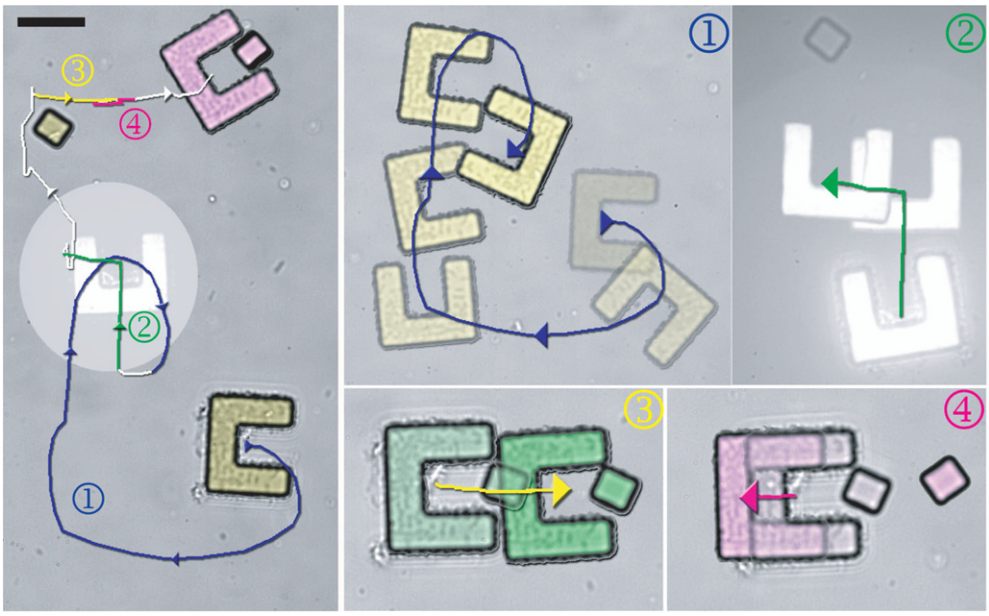

Figure 5. Movement of target loads. On the left is shown a summary of the complete path of an MBR transporter moving a target load described in detail in steps 1–4 (movie S4 available online at stacks.iop.org/JMM/21/035001/mmedia). The total time is 2 min, and the scale bar is 25 μm. (1) The transporter initially rotates clockwise due to the self-coordination of the bacterial carpet. Electric fields are applied to move the transporter to the left, and then up. (2) With the application of UV light, the transporter stops rotating in 6 s. As rotation is stopped, electric fields are applied to position the transporter close to the target. (3) The target is engaged and transported to the right. (4) The target is disengaged/reengaged by switching field polarity.

(figure 5). A self-rotating transporter was first positioned near the object by varying the direction of the electric field. Next, the transporter was stopped at an appropriate orientation to engage the target using localized UV light exposure. Once the rotational motion was stopped, the transporter was positioned to engage and move the load. The transporter was disengaged and reengaged by switching the polarity of the electric field.

These results suggest several potential applications for biological robotic systems. As demonstrated here, transport of microscale or even nanoscale objects is one application area. The dimensions of objects transported in these experiments are similar in scale to many types of living cells. These systems could also be employed for the assembly of small microparts.

2.4. Biosensing

Beyond purely mechanical tasks, MBRs may also be employed as mobile biosensors. In this section, we build on the previously developed techniques and demonstrate how changes in motility of MBRs in the presence of analytes can be used for biosensing using copper ions as an example. As the angular velocity of the MBRs is fully dependent on bacterial actuation, any significant change in the angular velocity will be understood as a change in the motility of attached bacteria, which points to the existence of the analyte. We monitor the changes in the motion of the MBRs and report directly on the activity of copper inside the chamber simply by visualization of their angular speed.

It has been shown that copper ions paralyze *S. marcescens* temporarily and in a reversible fashion [19]. Heavy metal ions directly bond to the rotor of the flagellar motor and impair its motion instantaneously. Adding chelating agents eliminates this effect as they form metal complexes. We carried out several experiments where we added different concentrations of $CuSO_4$ into the solution and the lowest copper ion concentration that our robots can detect was found to be 10 μM. The steady-state angular velocity of the devices decreases as the concentration of copper ions is increased from 10 to 100 μM. For concentration values higher than 100 μM, MBRs stopped moving immediately as expected and they started moving again with the addition of the chelating agent [19]. For the given concentration levels, exposure to copper does not damage the bacteria and the process can be repeated multiple times. As the MBRs stay on the same focal plane throughout the experiment, their motion can be recorded at all times.

Next, to demonstrate the ability to sense chemicals while scanning the whole control chamber with the MBRs, we designed a simple setup where we apply direct current electric fields in one dimension using a copper and a platinum electrode (figure 6(*a*)). MBRs were released into the central part of the experimental setup and an electric field of 10 V cm^{-1} was applied. Positively charged copper ions released from the anode migrated toward the negative electrode while negatively charged MBRs moved in the opposite direction. When MBRs encountered the copper ions, their motion due to bacterial actuation stopped immediately as the attached bacteria were paralyzed (figure 6(*b*)). The angular velocity became almost zero accordingly, as the main source of rotational motion of the MBRs is flagellar propulsion (figure 6(*c*)). The translational motion of the MBRs was slightly affected from copper. The contribution of the bacterial actuation to the translational velocity of the MBRs is small compared to their

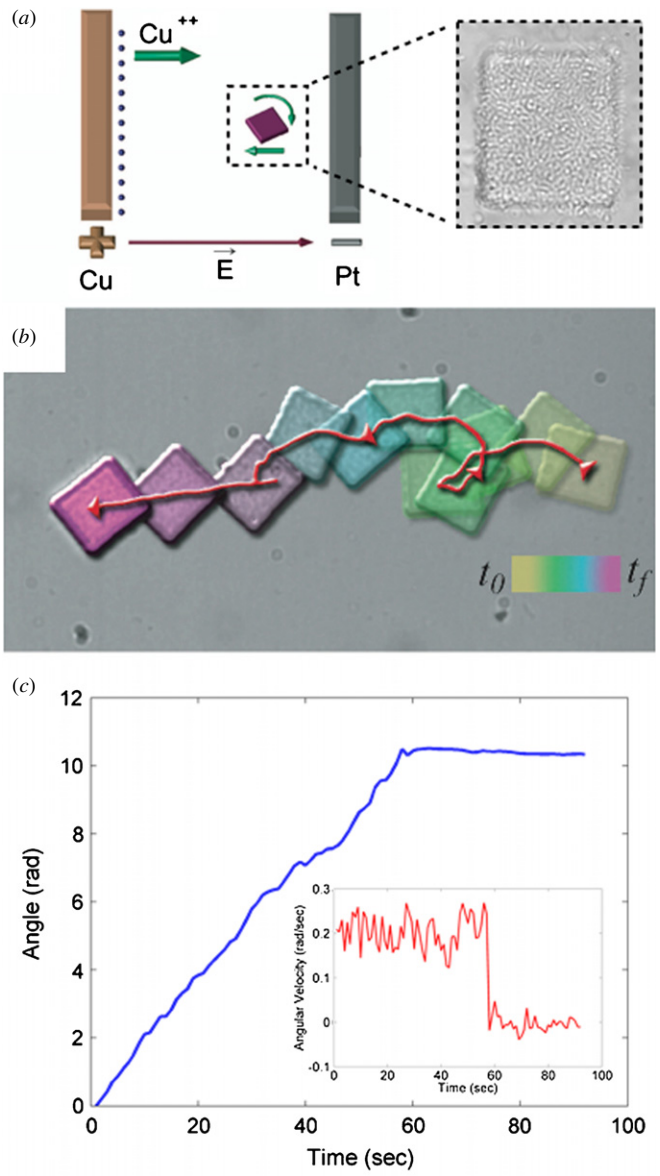

Figure 6. Biosensing. (*a*) Schematic of the setup used for the copper-sensing experiment. (*b*) Sensing of copper ions is observed as a loss of rotation. The translational movement due to the applied electric field persists (movie S5 available online at stacks.iop.org/JMM/21/035001/mmedia). (*c*) Angular position and velocity versus time. Scale bar represents time (100 s) as well as length (50 μm).

electrokinetic mobility. Starting from the robots closest to the positive electrode, all the robots inside the observation chamber stopped rotating one by one. We verified once again that the observed phenomenon was due to the released copper ions, by adding 0.01 M potassium phosphate into the solution. Potassium phosphate precipitates with copper and forms a visible compound. Heavy metal ions directly bond to the flagellar motor without initiating biochemical signals [19], but the method applied here can be extended to scenarios where chemical agents interact with chemoreceptors. Sensing capabilities of attached bacteria can also be extended by genetically engineering motility as a phenotypic response to other external stimuli [38].

The experimental framework that we develop in this paper is meant as a model system for other biological systems. We can extend our approach to use 'on-board' sensing combined with electrokinetic actuation to steer the MBRs to chemically or biologically relevant goals. With minimal fluid disturbance, using MBR biosensors in this fashion we can monitor signals in close proximity to target cells. While monitoring the local environment of target cells, we can simultaneously apply forces with the same microrobots. With appropriate genetic engineering, chemical signals could be generated to influence target cells. This technique may enable MBR–MBR communication by using genetically programmed sender and receiver cells [39].

3. Experimental details

3.1. Fabrication of parts

The SU-8 microfabrication and development procedure is compatible with a technique of release using a water-soluble sacrificial dextran layer [32]. Traditional techniques for the release of structures using a sacrificial layer required toxic chemicals. Using dextran for the release layer, the motility medium in which the studies are performed acted as an agent of release.

The chosen substrate for the patterning of SU-8 microstructures is glass. The fabrication sequence is shown in figure 1. The first spin-coating procedure was used to prepare a water-soluble sacrificial dextran layer. An aqueous solution of 5% (w/v) dextran 50–70 kDa was prepared by heating at 95 °C on a hot plate to enhance dissolution of the dextran into water. The solution was dispensed onto the glass slide and spin-coated at 3000 rpm for 15 s. The sacrificial layer was then baked for 2 min at 125 °C. Next, a 5 μm layer of SU-8 series 2 was spin-coated at 1000 rpm and pre-baked for 1 min at 65 °C and 3 min at 95 °C. The exposed substrate was post-baked and developed in PGMEA (SU-8 developer). The substrate was simply dried with nitrogen after PGMEA development.

3.2. Galvanotaxis chamber

We designed and fabricated a scalable experimental apparatus that we call a galvanotaxis chamber. Direct current electric fields were applied to the MBRs in this galvanotaxis chamber via agar salt bridges, Steinberg's solution (60 mM NaCl, 0.7 mM KCl, 0.8 mM $MgSO_4{\cdot}7H_2O$, 0.3 mM $CaNO_3{\cdot}4H_2O$) and graphite electrodes. It has been shown that salt bridges avoid contamination of possible electrode byproducts by successfully applying electric fields to a variety of cell types using similar galvanotaxis chambers [40]. The whole galvanotaxis chamber was fabricated on a glass plate out of polydimethylsiloxane (PDMS), a biocompatible material with well-known properties. This design was optimized to apply EFs efficiently in multiple directions. In order to minimize the possible adverse effects of electrode byproducts, we used graphite electrodes. The electrodes were fixed in parallel horizontal positions inside the compartments filled with Steinberg's solution to generate parallel EFs all over

the control chamber. The control chamber was filled with the motility buffer (0.01 M potassium phosphate, 0.067 M sodium chloride, 10^{-4} M ethylenediaminetetraacetic acid (EDTA) and 0.002% Tween-20, pH 7.0). Observations were performed in the central portion of the control chamber where dielectrophoretic effects due to field nonlinearities are minimized.

3.3. Data acquisition, analysis and feedback control

Imaging was performed on a Leica DMIRB inverted microscope with automated stage using phase contrast. Videos were captured using a high-speed camera (MotionPro X3, Redlake) with a frame rate of 30 frames s^{-1}. A simple tracking algorithm was designed to feedback the position and orientation of the MBR in the motility buffer. The control algorithm and the serial port connection protocol to interface with the programmable power supply for the electrodes were written in MATLAB 7.0. The optical path included a 100 W mercury light source and a 63× Fluorotar objective.

3.4. Cellular electrokinetics

A series of experiments were performed to characterize the effect of electric fields on the orientation of freely swimming *S. marcescens*. This study was performed to determine which electrokinetic phenomena cause directed movement of the MBRs. Upon application of electric fields in the range of 1–10 V cm^{-1} bacteria showed a uniform tendency to move toward the positive electrode; however, it was difficult to observe if the cells were orienting along electric field lines, as would be expected in the case of bacterial galvanotaxis. Due to the fact that preferential orientation may take several seconds to develop, 20 s were allowed to pass after electric fields were applied, but before images were taken. Between image acquisitions at discrete voltages, several seconds were allowed to pass to account for potential charging/discharging of the agar electrodes. Images were processed using MATLAB, and orientation was evaluated on a basis of 180° since the polarity of the flagellar bundle cannot be resolved using phase contrast microscopy.

4. Conclusions

In this work, we investigated and characterized the fundamental phenomena for controlling rotation and translation of engineered microscale structures using bacteria stimulated by UV light and electric fields. The electrokinetic phenomena were found to be primarily electrophoretic, with the primary component of MBR velocity related directly to the strength of the electric field. A custom-designed chamber was created to apply direct current electric fields in two dimensions, while also enabling continuous tracking and application of UV light. The photoresponsiveness of the cells was used to temporarily halt rotation of MBRs, downwardly adjust angular velocity, or permanently stop rotational motion, which was vital for the positioning of U-shaped microtransporters.

Examples of microscale transport and assembly as well as computer-based control of MBRs were presented. Potential applications include single cell manipulation, microassembly and biosensing. MBRs can be used as building blocks for more sophisticated functional microdevices. Furthermore, the paradigm introduced here can be integrated with other microelectromechanical systems (MEMS) technologies.

Acknowledgments

This work is partially supported by National Science Foundation CAREER grant CMMI-0745019, NSF grant CMMI-1000255 and ARO MURI SWARMS grant W911NF.

References

[1] Weibel D B, DiLuzio W R and Whitesides G M 2007 Microfabrication meets microbiology *Nat. Rev. Microbiol.* **5** 209–18
[2] Abbott J J, Nagy Z, Beyeler F and Nelson B J 2007 Robotics in the small: part I. Microbotics *Robot. Autom. Mag. IEEE* **14** 92–103
[3] Chiou P Y, Ohta A T and Wu M C 2005 Massively parallel manipulation of single cells and microparticles using optical images *Nature* **436** 370–2
[4] Yi C, Li C-W, Ji S and Yang M 2006 Microfluidics technology for manipulation and analysis of biological cells *Anal. Chim. Acta* **560** 1–23
[5] Desai J P, Pillarisetti A and Brooks A D 2007 Engineering approaches to biomanipulation *Annu. Rev. Biomed. Eng.* **9** 35–53
[6] Castillo J, Dimaki M and Svendsen W E 2009 Manipulation of biological samples using micro and nano techniques *Integr. Biol.* **1** 30–42
[7] Purcell E M 1976 Life at low Reynolds number *Am. J. Phys.* **45** 3–11
[8] Dreyfus R, Roper M L, Stone H A and Bibette J 2005 Microscopic artificial swimmers *Nature* **437** 862–5
[9] Zhang L, Abbott J J, Dong L, Kratochvil B E, Bell D and Nelson J 2009 Artificial bacterial flagella: fabrication and magnetic control *Appl. Phys. Lett.* **94** 064107
[10] Ghosh A and Fischer P 2009 Controlled propulsion of artificial magnetic nanostructured propellers *Nano Lett.* **9** 2243–6
[11] Garstecki P, Tierno P, Weibel D B and Sagues F 2009 Propulsion of flexible polymer structures in a rotating magnetic field *J. Phys.: Condens. Matter* **21** 204110
[12] Fahrni F, Prins M W J and van IJzendoorn L J 2009 Micro-fluidic actuation using magnetic artificial cilia *Lab Chip* **9** 3413–21
[13] Zhang L, Peyer K E and Nelson B J 2010 Artificial bacterial flagella for micromanipulation *Lab Chip* **10** 2203–15
[14] Heuvel M G L and Dekker C 2007 Motor proteins at work for nanotechnology *Science* **317** 333–6
[15] Feinberg A W, Feigel A, Shevkoplyas S S, Sheehy S, Whitesides G M and Parker K K 2007 Muscular thin films for building actuators and powering devices *Science* **317** 1366–70
[16] Hiratsuka Y, Miyata M, Tada T and Uyeda T Q P 2006 A microrotary motor powered by bacteria *Proc. Natl Acad. Sci.* **103** 13618
[17] Darnton N, Turner L, Breuer K and Berg H C 2004 Moving fluid with bacterial carpets *Biophys. J.* **86** 1863–70
[18] Martel S, Tremblay C C, Ngakeng S and Langlois G 2006 Controlled manipulation and actuation of micro-objects with magnetotactic bacteria *Appl. Phys. Lett.* **89** 233904
[19] Behkam B and Sitti M 2007 Bacterial flagella-based propulsion on/off motion control of microscale objects *Appl. Phys. Lett.* **90** 023902

[20] Steager E, Kim C-B, Patel J, Bith S, Naik C, Reber L and Kim M J 2007 Control of microfabricated structures powered by flagellated bacteria using phototaxis *Appl. Phys. Lett.* **90** 263901
[21] Weibel D B, Garstecki P, Ryan D, DiLuzio W R, Mayer M, Seto J E and Whitesides G M 2005 Microoxen: microorganisms to move microscale loads *Proc. Natl Acad. Sci.* **102** 11963–7
[22] Nagai M, Ryu S, Thorsen T, Matsudaira P and Fujita H 2010 Chemical control of *Vorticella* bioactuator using microfluidics *Lab Chip* **10** 1574–8
[23] Voigt C A 2006 Genetic parts to program bacteria *Curr. Opin. Biotechnol.* **17** 548–57
[24] Cerf A, Cau J-C, Vieu C and Dague E 2009 Nanomechanical properties of dead or alive single-patterned bacteria *Langmuir* **25** 5731–6
[25] Kim M J and Breuer K S 2008 Self-organizing bacteria-powered microfluidic pumps *Small* **4** 111–8
[26] Kim M and Breuer K 2007 Controlled mixing in microfluidic systems using bacterial chemotaxis *Anal. Chem.* **79** 955–9
[27] Sokolov A, Apodaca M M, Grzybowski B A and Aranson I S 2010 Swimming bacteria power microscopic gears *Proc. Natl Acad. Sci.* **107** 969–74
[28] Di Leonardo R, Angelani L, Dell'Arciprete D, Ruocco G, Iebba V, Schippa S, Conte M P, Mecarini F, De Angelis F and Di Fabrizio E Bacterial ratchet motors *Proc. Natl Acad. Sci.* **107** 9541–5
[29] Julius A A, Sakar M S, Steager E B, Cheang U K, Kim M-J, Kumar V and Pappas G J 2009 Harnessing bacterial power for microscale manipulation and locomotion *2009 IEEE Int. Conf. on Robotics and Automation (Kobe, Japan)* pp 1004–9
[30] Alberti L and Harshey R M 1990 Differentiation of *Serratia marcescens* 274 into swimmer and swarmer cells *J. Bacteriol.* **172** 4322–8
[31] Murray P R, Rosenthal K S, Kobayashi G S and Pfaller M A 2002 *Medical Microbiology* (London: Mosby)
[32] Linder V, Gates B D, Ryan D, Parviz B A and Whitesides G M 2005 Water-soluble sacrificial layers for surface micromachining *Small* **1** 730
[33] Sokolov A, Aranson I S, Kessler J O and Goldstein R E 2007 Concentration dependence of the collective dynamics of swimming bacteria *Phys. Rev. Lett.* **98** 158102
[34] Shi W, Stocker B A D and Adler J 1996 Effect of the surface composition of motile *E. coli* and motile *Salmonella* on the direction of galvanotaxis *J. Bacteriol.* **178** 1113–9
[35] Taylor B L and Koshland D E 1975 Intrinsic and extrinsic light responses of *Salmonella typhimurium* and *Escherischia coli* *J. Bacteriol.* **123** 557–69
[36] Kim D H, Steager E B, Cheang U K, Byun D and Kim M-J 2010 Comparison of contour based and feature based tracking methods for control of microbiorobots *J. Micromech. Microeng.* **20** 065006
[37] Macnab R and Koshland D E 1974 Bacterial motility and chemotaxis: light-induced tumbling response and visualization of individual flagella *J. Mol. Biol.* **85** 399–406
[38] Weiss L E, Badalamenti J P, Weaver L J, Tascone A R, Weiss P S, Richard T L and Cirino P C 2008 Engineering motility as a phenotypic response to LuxI/R-dependent quorum sensing in *Escherichia coli Biotechnol. Bioeng.* **100** 1251–5
[39] Basu S, Gerchman Y, Collins C H, Arnold F H and Weiss R 2005 A synthetic multicellular system for programmed pattern formation *Nature* **434** 1130–4
[40] Song B, Gu Y, Pu J, Reid B, Zhao Z and Zhao M 2007 Application of direct current electric fields to cells and tissues *in vitro* and modulation of wound electric field *in vivo Nat. Protoc.* **2** 1479–89